

Sizing Optimization of Truss Structures using a Hybridized Genetic Algorithm

November 28, 2016

Reza Najian Asl^{*}, ¹, Research Assistant
Mohamad Aslani, ², Research Assistant
Masoud Shariat Panahi ³, Associate Professor

arXiv:1306.1454v1 [math.OC] 6 Jun 2013

¹*Corresponding author: Research Assistant, Mechanical Engineering Department, University of Tehran, Tehran, Iran. reza.najian-asl@tum.de

²Research Assistant, Mechanical Engineering Department, University of Tehran, Tehran, Iran. maslani@iastate.edu

³Mechanical Engineering Department, University of Tehran, Tehran, Iran. mshariatp@ut.ac.ir

Abstract

This paper presents a genetic-based hybrid algorithm that combines the exploration power of Genetic Algorithm (GA) with the exploitation capacity of a phenotypical probabilistic local search algorithm. Though not limited to a certain class of optimization problems, the proposed algorithm has been “fine tuned” to work particularly efficiently on the optimal design of planar and space structures, a class of problems characterized by the large number of design variables and constraints, high degree of non-linearity and multitude of local minima. The proposed algorithm has been applied to the skeletal weight reduction of various planar and spatial trusses and shown to be superior in all of the cases.

Keywords: Truss Structures, Optimal Design, Hybrid Search Strategies, Genetic Algorithms

1 Introduction

Skeletal structures are widely used as benchmark test in structural optimization as they can include a large number of design variables and constraints leading to high degree of non linearity and presence of local minima. The demand for reliable, computationally inexpensive optimum structural design tools has motivated the researchers to develop specialized optimization techniques and/or to “tune” existing methods to solve this class of problems more efficiently. Structural design problems are typically characterized by their large numbers of design variables and constraints, high degree of non-linearity and multitude of local minima. It is therefore extremely difficult, if not practically impossible, to find the globally optimum solution to the problem of designing large scale space structures unless some additional knowledge of the optimum’s whereabouts is available to guide the search. If this specific knowledge is not available, one has to resort to search techniques that can, to a certain extent, escape the local minima and spot the global one(s). It comes with no surprise that structural optimization has grown to become a challenging one, seeking to determine the structure’s dimensions, geometry and topology that would render the structure as light/inexpensive as possible while keeping its performance characteristics (e.g. stresses and displacements) within allowable limits. The inherent complexity of the problem has rendered it a perfect benchmark for large scale search algorithms.

It is widely believed that Evolutionary Algorithms (EAs) are so far the most promising methods for searching large, highly non-linear design space black box problems with many local minima. EAs are stochastic search methods that mimic the metaphor of natural biological evolution. They operate on a population of potential solutions applying the principle of survival of the fittest to produce increasingly better approximations to a solution. Through the adaptation of successive generations of a large number of individuals, an evolutionary algorithm performs an efficient directed search. Evolutionary search is generally better than random search and is not susceptible to the hill-climbing behaviours of gradient-based search [1].

The most common EA is Genetic Algorithm (GA) that was introduced by Holland in 1975 [2]. In Holland’s view, GAs are a computational analogy of adaptive systems. They are modelled loosely on the principles of the evolution via natural selection, employing a population of individuals that undergo selection in the presence of variation-inducing operators such as mutation and recombination(crossover). A fitness function is used to evaluate individuals, and reproductive success varies with fitness [1]. From a practical point of view, traditional GAs suffer from two problems: their high computational cost and their vulnerability to getting trapped in local minima of the objective function, especially when the number of variables is large and/or the design space is bounded with a huge number of constraints. Many modifications have been performed on the operators of GAs to resolve these problems, most of them aimed at changing GAs to increase their rate of convergence. A more recent trend has been to hybridize GAs with other, more specialized, optimization techniques such as Simulated Annealing (SA) [3] and [4], Nelder-Mead(Simplex) [5], [6] and [7] and Monte Carlo algorithm [8] and particle swarm optimizer [9].

Since the standard GA operators are traditionally unable to secure a local search in the neighbourhood of existing solutions, it might be argued that hybridization of GA with a neighbourhood search algorithm would improve its convergence rate. However, this neighbourhood search algorithm must not undermine the stochastic nature of GA and must be justifiably simple so that that the resulting hybrid algorithm would not border with a simple random walk in the design space. These conditions make SA a prime candidate for the job; a simple, yet powerful stochastic search algorithm that is not fooled by false minima and is easy to implement. However, Simulated Annealing, even after recent improvements aimed at boosting its convergence behaviour [10], comes with its own drawbacks, including its high sensitivity to the location of initial points. The farther from the global optimum they are, the more iteration it takes the algorithm to get there. This is because the static neighbourhood search of the SA(one with a constant neighbourhood radius throughout the search) makes the algorithm unable to adjust its neighbourhood size according to its distance from the optimum. This could be avoided by introducing a “dynamic” neighbourhood search where the radius of the local search area is adaptively varied according to some measure of “closeness” to the global optimum. In the next section, a new hybrid GA is introduced which adopts a modified version of SA’s stochastic neighbourhood search to improve its convergence rate. Then back to our structural sizing optimization problem and it is shown that how the problem could be solved using the proposed algorithm.

2 The Hybrid Simulated Annealing-Genetic Algorithms(H-SAGA)

In order to clarify nomenclature, the basis of GA and SA algorithms included in the present optimization code will be briefly recalled.

2.1 The Basic Genetic Algorithm

In a Genetic Algorithm, a predetermined number(a population) of strings(chromosomes) which encode candidate solutions to an optimization problem evolves toward better solutions. Actual solutions(phenotype) are represented by

(binary/real value) encoded strings(genotype). The evolution usually starts from a population of randomly generated individuals and happens in generations. In each generation, the fitness(measure of desirability) of every individual in the population is evaluated.

Multiple individuals are then stochastically selected from the current population (based on their fitness), and modified using such genetic operators as recombination(cross over) and mutation to form a new population. The new population is then used as the “current population” in the next iteration of the algorithm.

The population size depends on the nature of the problem. While a large population size tends to secure the diversity of the candidate solutions and avoids a premature convergence, it inevitably increases the computational cost of the search. Special arrangements are usually made to encourage a relatively uniform distribution of individuals across the search space. Occasionally, the solutions may be “seeded” in areas where optimal solutions are likely to be found.

To breed a new generation, individual solutions are selected to form a “mating pool” through a fitness based process, where fitter solutions (as measured by a fitness function) would have a higher chance to be selected. In GA the selection mechanism is always partially (if not totally) stochastic to allow some proportion of less fit solutions be possibly selected. This helps keep the diversity of the population large, preventing premature convergence to poor solutions.

For each new solution to be produced, a pair of “parent” solutions is selected for breeding from the mating pool. By producing a “child” solution using genetic operators, a new solution is created which typically shares many of the characteristics of its “parents”. New parents are selected for each new child, and the process continues until a new population of solutions of appropriate size is generated. The average fitness of the new generation is expected to be higher than that of the previous generation, as the best individuals of the last generation have been given higher chances for breeding.

The algorithm terminates when either a maximum number of generations has been produced, or a satisfactory fitness level has been reached for the population.

2.2 The Basic Simulated Annealing

Initially developed in the field of statistical mechanics to simulate a collection of atoms in equilibrium at a given temperature[11], Simulated Annealing was soon recognized as a powerful optimization technique. The name and inspiration come from the “annealing” process in metallurgy, a technique involving heating and controlled cooling of a material to increase the size of its crystals and reduce their defects. The heat causes the atoms to become unstuck from their initial positions(a local minimum of the internal energy) and wander randomly through states of higher energy; the slow cooling gives them more chances of finding configurations with lower internal energy than the initial one. By analogy with this physical process, each step of the SA algorithm replaces the current solution(A) by a random “nearby” solution(B), generated within a neighbourhood of predetermined size, with a probability(P) that depends on the difference between the corresponding function values and on a global parameter T (called the temperature), that is gradually decreased during the process. This probability, in its basic form, is calculated as follows:

$$P = \begin{cases} 1(i.e. 100\%) & \text{if } f(A) \geq f(B) \\ \exp(\frac{f(A)-f(B)}{T}) & \text{otherwise} \end{cases} \quad (1)$$

This formula(Eq.2) is commonly justified by analogy with the transitions of a physical system. The essential property of this probability function is that it is non zero when $f(B) \geq f(A)$, meaning that the system may move to the new state even when it is worse (has a higher energy) than the current one. It is this feature that prevents the algorithm from becoming stuck in a local minimum (a state that is worse than the global minimum, yet better than any of its neighbours).

The algorithm terminates when either the temperature falls below a certain value or the objective function does not improve much during a certain number of consecutive iterations. As mentioned earlier, an improved SA formulation will be used in which the neighbourhood of local search is adaptively re-sized throughout the search.

2.3 Handling Constraints

A constrained problem in which the feasible region is defined by a set of implicit/explicit constraints could be treated in two ways. One is to use them as preventive measures that would not allow a newly generated solution to enter the population unless it satisfies all the constraints; and the other is to use them as penalizers, that is to allow infeasible solutions to enter the population but penalize (increase, in case of a minimization problem) their fitness in proportions with their degree of constraint violation. The latter is usually preferred because it provides the user with a quantitative measure of the infeasibility of a solution and helps the algorithm find its way to the feasible region.

In structural optimization, weight of the structure usually constitutes the objective function and cross-sectional properties of the members form the variable set. Also, the structure is constrained in terms of the stresses and displacements of its members. These are considered indirect constraints as they are not applied directly on the cross sections of the members.

These non-linear constraints are incorporated into the objective function to form a new, unconstrained function. In this way, infeasible solutions are given a varying amount of penalty to subside their fitness. In an attempt to make the search somewhat adaptive, dynamic penalties are introduced that would vary with the number of iterations. The problem could then be formulated as follows (without loss of generality, only the inequality constraints are considered

here):

$$\begin{aligned}
& \text{minimize} && f(\mathbf{x}) \\
& \text{with respect to} && \mathbf{x} = (x_1, \dots, x_n) \\
& \text{subject to} && g_i(\mathbf{x}) \leq 0, \forall i = 1 \text{ to } m
\end{aligned} \tag{2}$$

The new, unconstrained objective function would then be defined as:

$$F(\mathbf{x}) = f(\mathbf{x}) \pm p(\mathbf{x}) \tag{3}$$

where

$$p(\mathbf{x}) = \alpha(\#iteration)^\beta \times \sum_{i=0}^q S_i(\mathbf{x}) \tag{4}$$

and

$$S_i(\mathbf{x}) = \begin{cases} 0 & g_i(\mathbf{x}) \leq 0 \\ \|g_i(\mathbf{x})\| & otherwise \end{cases} \tag{5}$$

2.4 The Dynamic Neighbourhood Search (DNS)

To accelerate the search and reduce the number of times the algorithm falls into and climbs out of local valleys (in a minimization problem), the neighbourhood of local search for each design variable is initially set equal to the difference between its highest and lowest values within the 10 best individuals, a large value meant to encourage exploratory leaps. The neighbourhood is then progressively reduced using an improvement-dependent criterion aimed at refining the search steps once large exploratory steps could no longer improve the solution. The performance of DNS is controlled by two user-defined parameters: the radius reduction threshold β and the contraction parameter γ . The implementation of DNS is somewhat elaborated in the pseudo code below.

2.5 The Hybrid Algorithm

In essence, the proposed hybrid algorithm works as follows:

- An initial population of encoded potential solutions is randomly generated (this may contain infeasible solutions);
- Fitness of each solution is calculated using the alternative objective function (Eq. 3);
- The population is evolved according to GA;
- Every T_{SA} (Simulated Annealing Threshold) generations, a SA search is performed with its initial point set at the fittest individual in generation T_{SA} . The search region is defined by current positions of the 10 fittest solutions in generation T_{SA} and the size of the neighbourhood to be locally searched is calculated according to section 2.4. The SA search is terminated once the average fitness improvement within a certain number of consecutive iterations falls below a search precision (ϵ) and or the temperature falls below a predefined value (T_{MIN}) implying that further probabilistic moves to inferior neighbouring points would be highly unlikely;
- For every new solution suggested by SA, an individual is removed from the population with a probability proportional to the inverse of its fitness;
- The algorithm terminates once the termination criteria for the GAs is met;

A pseudo code for the algorithm is presented below:

```

Choose GA parameters, radius reduction threshold (TSA)
Generate initial population (randomly)
Do
    Evaluate each individual's constraint violation (Eq. 4)
    Evaluate unconstrained objective function (Eq. 3)
Form the new generation
    Use fitness-proportionate selection to form the mating pool
    Mate pairs at random
    Apply crossover operator
    Apply mutation operator
    Rank individuals based on their fitness
    Select 10 best-ranking individuals
    If number of generations since last application of SA equals  $T_{SA}$ 
        Apply SA
        Define an initial temperature  $T$ 
        Set the search radius of each design variable ( $R_i$ ) (Section 2.4)
        Choose the cooling coefficient  $\alpha$  ( $0 < \alpha < 1$ )
        Choose radius reduction threshold  $\beta$  and the contraction parameter  $\gamma$ 
        Choose the top-ranking individual as the starting point
        Do
            Choose a random point ( $N$ ) in the neighbourhood of current point( $C$ )

```

Set $\delta = f(P) - f(C)$
If $\delta < 0$ by probability P (Eq. 2)
Replace C with N
If number of SA iterations equals number of design variables $T = \alpha T$
Endif
If iterations falls below β
Then upgrade search radius $R_{(i,new)} = R_{(i,old)}/\gamma$
Endif
While SA termination criteria met (Section 2.5)
Add SA solution to the population and remove an individual based on the inverse of their fitness
Endif
While GA termination criteria is met

3 Application to Structural Design Problems

A variety of structural design problems ranging from a 10-bar planar truss to a 26-story space structure with various numbers of variables and constraints are considered in this section.

From an analytical point of view, the problem of weight minimization of a truss structure is defined as:

$$\begin{aligned}
 & \text{minimize} \quad W(\mathbf{A}) = \rho g \sum_{j=1}^{NEL} A_j l_j \\
 & \text{with respect to} \quad \mathbf{A} = (A_1, \dots, A_{NEL}) \\
 & \text{subject to} \quad \begin{cases} u_{(x,y,z),k}^l \leq u_{(x,y,z),k,ilc} \leq u_{(x,y,z),k}^u \\ \sigma_j^l \leq \sigma_{j,ilc} \leq \sigma_j^u \\ A_j^l \leq A_j \leq A_j^u \end{cases} \quad \begin{cases} i = 1, NEL \\ k = 1, NOC \\ l = 1, NLC \end{cases} \quad (6)
 \end{aligned}$$

Where:

- A_i are the cross sectional areas of the members;
- W is the total weight of the structure;
- NEL is the number of elements in the structure;
- NOD is the total number of nodes;
- NLC is the number of independent loading conditions acting on the structure;
- g is the gravity acceleration;
- ρ is the material density used in the structure;
- \mathbf{A} is the vector of the cross sectional area values; A_j is the j_{th} element area of the structure.
- A_j^l and A_j^u are lower and upper bounds of A_j ;
- l_j is the length of j_{th} element, and is calculated according to Eq. 8;

$$l_j = \sqrt{(x_{j1} - x_{j2})^2 + (y_{j1} - y_{j2})^2 + (z_{j1} - z_{j2})^2} \quad (7)$$

where $x_{j1,2}, y_{j1,2}, z_{j1,2}$ are coordinates of the nodes of the j_{th} element;

- $u_{(x,y,z),k,ilc}$ is the displacement of the k_{th} node in the directions x, y, z with the lower and upper limits $u_{(x,y,z),k}^l$ and $u_{(x,y,z),k}^u$ in corresponding of the ilc_{th} loading condition, Eq. 6;
- $\sigma_{j,ilc}$ is the stress on the j_{th} element, σ_k^l and σ_k^u are the lower and upper limits in correspondence of the ilc_{th} loading condition, Eq.6;

Design variables (A_i) are treated as continuous variables, as it is a common practice in the literature. Each truss structure is analysed using the *FEM displacement method* and the results are presented in a separate table. Attention must be paid to the fact that the numbers reported in these tables have been rounded up to 4 digits. They may therefore seem to slightly violate some of the constraints or deviate from global optimality, a problem that does not arise when the actual, 7-digit values are considered.

3.1 The 10-bar truss

The cantilever truss shown in Fig. 1 with 10 independent design variables has been studied by many researchers Schmit and Farshi [12], Schmit and Miura [13], Venkayya [14], Sedaghati [15], Kaveh and Rahami [16], Li et al. [17], Farshi and Ziazi [17], Rizzi [18], John et al. [19]. A material density of $0.1lb/(in^3)$ and a modulus of elasticity of $10000ksi$ is commonly used. Members are constrained in displacement and stress to $\pm 2in$ and $\pm 25ksi$ respectively. The lower bound of cross sectional areas is $0.1in^2$. Two load cases are considered (Fig.1):

1. A single load ($P_1 = 100kips$ and $P_2 = 0kips$)
2. Double loads ($P_1 = 150kips$ and $P_2 = 50kips$)

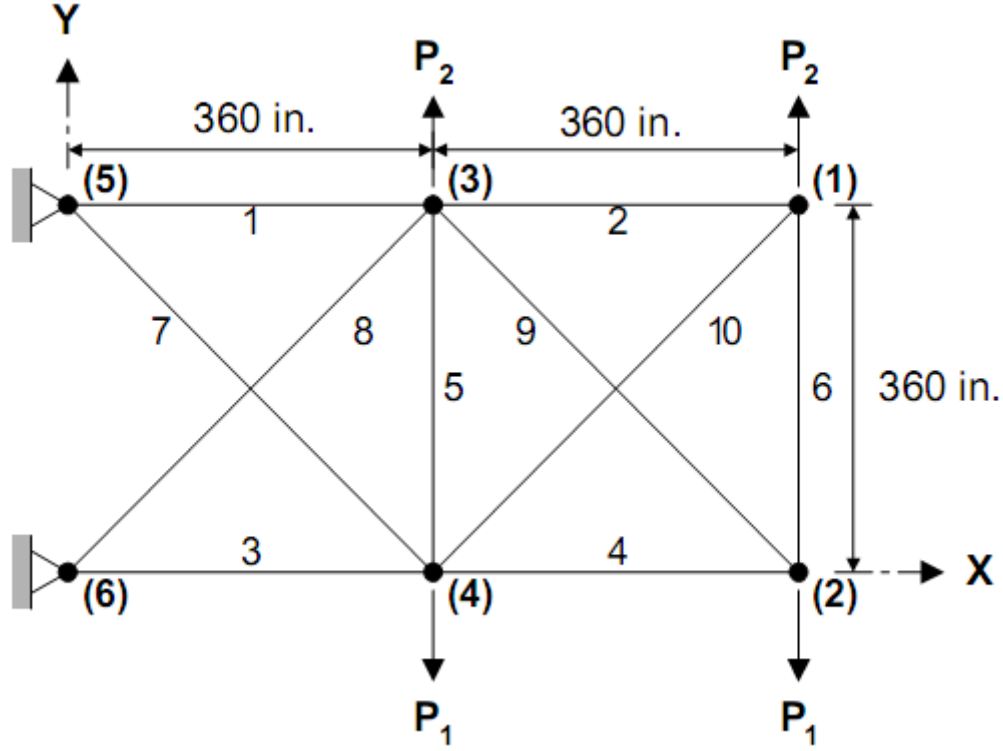


Figure 1: 10-bar planar truss

Table 1: Optimal design comparison for the 10-bar planar truss (Case 1)

Variables(in^2)	Schmit and Farsh [12]	Schmit and Miura [13]	Venkayya [14]	Sedaghati [15]	Kaveh and Rahami [16]	Li et al. [17]	Farshi and Ziazi [21]	This work
A_1	33.43	30.67	30.42	30.5218	30.6677	30.704	30.5208	30.5091
A_2	0.100	0.100	0.128	0.1000	0.1	0.100	0.1000	0.1000
A_3	24.26	23.76	23.41	23.1999	22.8722	23.167	23.2040	23.2004
A_4	14.26	14.59	14.91	15.2229	15.3445	15.183	15.2232	15.1926
A_5	0.100	0.100	0.101	0.1000	0.1	0.100	0.1000	0.1000
A_6	0.100	0.100	0.101	0.5514	0.4635	0.551	0.5515	0.5559
A_7	8.388	8.578	8.696	7.4572	7.4796	7.460	7.4669	7.4612
A_8	20.74	21.07	21.08	21.0364	20.9651	20.978	21.0342	21.0714
A_9	19.69	20.96	21.08	21.5284	21.7026	21.508	21.5294	21.4731
A_{10}	0.100	0.100	0.186	0.1000	0.1	0.100	0.1000	0.1000
Weight lb	5089.0	5076.85	5084.9	5060.85	5061.90	5060.92	5061.4	5058.66

Note: $1 in^2 = 6.425cm^2$ $1lb = 4.448N$

Tables 1 and 2 give the optimum design for Cases 1 and 2, respectively, and also provide a comparison between the optimal design results reported in the literature and the present work¹.

3.2 The 17-bar truss

The 17-bar truss of Fig. 2 is also a typical test case studied by many researchers, including Khot and Berke [22], Adeli and Kumar [23], Lee and Geem [20]. In this case the material density is $0.268lb/in^3$ and the modulus of elasticity is $30000ksi$. A displacement limitation of $\pm 2in$ were the only constraint that imposed on the nodes in both x and y directions. A single loading of $100kips$ is on the node (9), Seventeen independent variables exist as there is no variable grouping in the problem. A minimum cross-section of $0.1in^2$ is the lower boundary of the variables.

Table 3 compares the optimization results with similar studies published in literature. It can be seen that H-SAGA

¹The results included here and in the rest of this paper for comparison purposes are the “feasible” ones. A few reported solutions that involve constraint violation(s), including those reported in references [17] and [20] are not included for some cases here.

Table 2: Optimal design comparison for the 10-bar planar truss (Case 2)

Variables(in^2)	Schmit and Farsh [12]	Schmit and Miura [13]	Venkayya [14]	Rizzi [18]	John et al. [19]	Lie et al. [17]	Farshi and Ziazi [21]	This work
A_1	24.29	23.55	25.19	23.53	23.59	23.353	23.5270	23.3187
A_2	0.100	0.100	0.363	0.100	0.10	0.100	0.1000	0.1
A_3	23.35	25.29	25.42	25.29	25.25	25.502	25.2941	25.5790
A_4	13.66	14.36	14.33	14.37	14.37	14.250	14.3760	14.6640
A_5	0.100	0.100	0.417	0.100	0.10	0.100	0.1000	0.1
A_6	1.969	1.970	3.144	1.970	1.97	1.972	1.9698	1.9695
A_7	12.67	12.39	12.08	12.39	12.39	12.363	12.4041	12.2654
A_8	12.54	12.81	14.61	12.83	12.80	12.894	12.8245	12.6473
A_9	21.97	20.34	20.26	20.33	20.37	20.356	20.3304	20.3422
A_{10}	0.100	0.100	0.513	0.100	0.10	0.101	0.1000	0.1
Weight lb	4691.84	4676.96	4895.60	4676.92	4676.93	4677.29	4677.8	4675.43

Note: $1 in^2 = 6.425cm^2$ $1lb = 4.448N$

Table 3: Optimal design comparison for the 17-bar planar truss

Variables(in^2)	Khot and Berke [22]	Adeli and Kumar [23]	Lee and Geem [20]	This work
A_1	15.93	16.029	15.821	15.8187
A_2	0.1	0.107	0.108	0.1051
A_3	12.07	12.183	11.996	12.0246
A_4	0.1	0.1	0.1	0.1
A_5	8.067	8.417	8.15	8.1132
A_6	5.562	5.715	5.507	5.5318
A_7	11.933	11.331	11.829	11.8431
A_8	0.1	0.105	0.1	0.1
A_9	7.945	7.301	7.934	7.9560
A_{10}	0.1	0.115	0.1	0.1
A_{11}	4.055	4.046	4.093	4.0711
A_{12}	0.1	0.101	0.1	0.1
A_{13}	5.657	5.611	5.66	5.6841
A_{14}	4	4.046	4.061	4.0087
A_{15}	5.558	5.152	5.656	5.5849
A_{16}	0.1	0.107	0.1	0.1
A_{17}	5.579	5.286	5.582	5.5804
Weight lb	2581.89	2594.42	2580.81	2578.76

Note: $1 in^2 = 6.425cm^2$ $1lb = 4.448N$

designed a lighter structure.

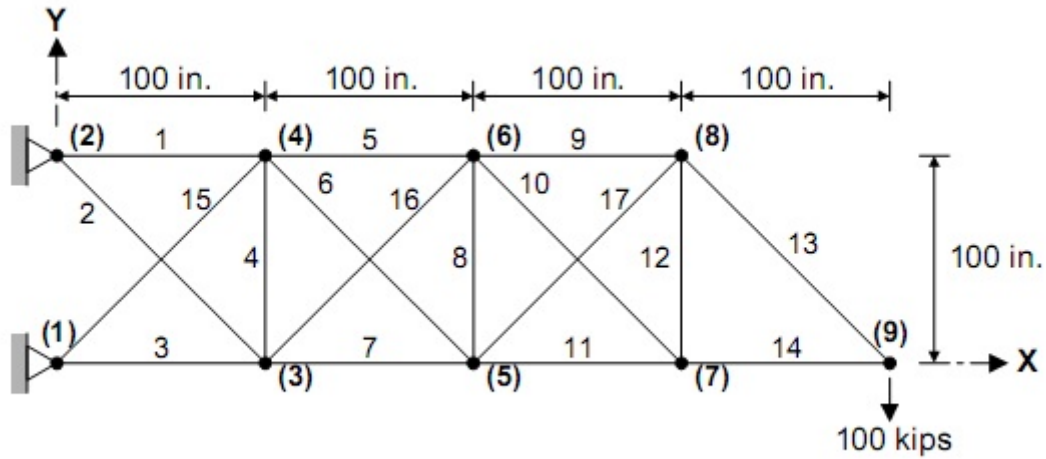


Figure 2: 17-bar planar truss

3.3 The 18-bar truss

The optimum design of the 18-bar cantilever truss shown in Fig.3 is a sizing optimization problem already analyzed by Imai and Schmit [24] and Lee and Geem [20]. Material density is $0.1lb/(in^3)$. Stress in members must not exceed $20000psi$ (The same limit in tension and compression). Constraints on Euler buckling strength are also considered where the allowable limit for the i th member is computed as:

$$\sigma_i^b = -\frac{KEA_i}{L_i^2} \quad (8)$$

where K is the buckling constant ($K = 4$). E is the modulus of elasticity ($E = 10000ksi$) and L_i is the length of the element. Downward load of $F = 20kips$ is on nodes (1), (2), (4), (6) and (8). The member cross-section groups are as follow:

1. $A_1 = A_8 = A_{12} = A_4 = A_{16}$
2. $A_2 = A_6 = A_{10} = A_{14} = A_{18}$
3. $A_3 = A_7 = A_{11} = A_{15}$
4. $A_5 = A_9 = A_{13} = A_{17}$

Minimum cross section is $0.1in^2$. H-SAGA obtained a lighter designing in comparison with other algorithms. These results are presented in Table 4.

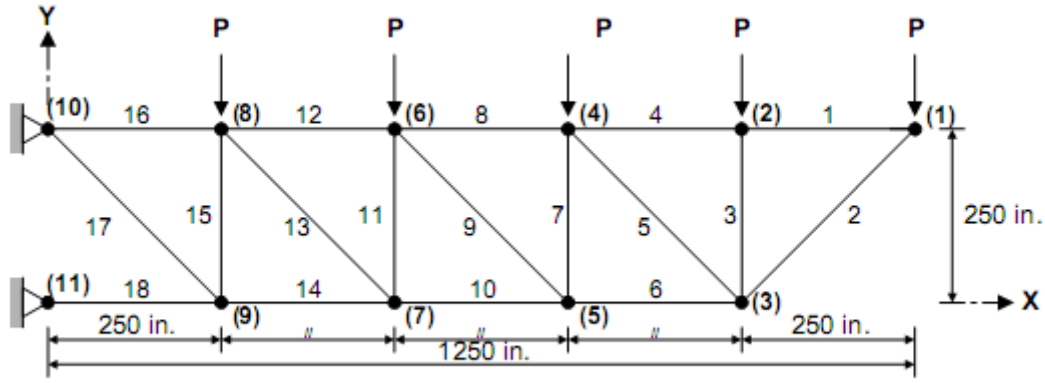


Figure 3: 18-bar planar truss

Table 4: Optimal design comparison for the 18-bar planar truss

Variables(in^2)	Imai and Schmit [24]	Lee and Geem [20]	This work
A_1	9.998	9.98	9.9671
A_2	21.65	21.63	21.5990
A_3	12.5	12.49	12.4492
A_4	7.072	7.057	7.0490
Weight lb	6430	6421.88	6419.23

3.4 The 22-bar space truss

Weight minimization of the spatial 22-bar truss shown in Fig.4 was previously attempted with or without layout variables by Sheu and Schmit [25], Khan and Willmert [26], Li et al [17], Farshi and Ziazi [21]. Material density was taken as $0.1lb/in^3$, the modulus of elasticity as $10000psi$. Members were grouped as follows:

(1) $A_1 \sim A_4$ (2) $A_5 \sim A_6$ (3) $A_7 \sim A_8$ (4) $A_9 \sim A_{10}$ (5) $A_{11} \sim A_{14}$ (6) $A_{15} \sim A_{18}$ (7) $A_{19} \sim A_{22}$ Stress members are limited

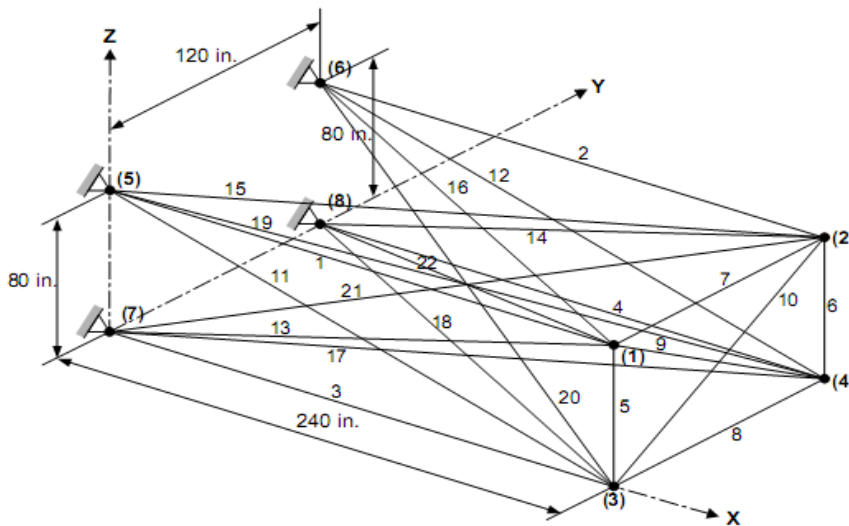


Figure 4: 22-bar space truss

according to Table 5. Nodal displacement must be less than $2in$. The structure is subject to three independent loading conditions (Table 6). The lower bound of cross sectional areas is $0.1in^2$. Optimization results are presented in Table 7.

3.5 The 25-bar space truss

The 25-bar tower space truss of Fig.5 has been analyzed by many researchers, including Schmit and Farshi [12], Schmit and Miura [13], Venkayya [14], Adeli and Kamal [27], Saka [28], Lamberti [29], Farshi and Ziazi [21]. In these studies, the material density is $0.1lb/in^3$ and modulus of elasticity is $10000ksi$. This space truss is subjected to the two loading conditions shown in Table 8. The cross section grouping is as follows: (1) A_1 (2) $A_2 \sim A_5$ (3) $A_6 \sim A_9$ (4) $A_{10} \sim$

Table 5: Stress limits for the spatial 22-bar truss problem

Variables(in^2)	Grouping	Compressive Stress Limitation (ksi)	Tensile stress limitation(ksi)
1	$A_1 \sim A_4$	24.0	36.0
2	$A_5 \sim A_6$	30.0	36.0
3	$A_7 \sim A_8$	28.0	36.0
4	$A_9 \sim A_{10}$	26.0	36.0
5	$A_{11} \sim A_{14}$	22.0	36.0
6	$A_{15} \sim A_{18}$	20.0	36.0
7	$A_{19} \sim A_{22}$	18.0	36.0

Table 6: Loading conditions for the 22-bar space truss

Node	Loading Condition 1(psi)	Loading Condition 2(psi)	Loading Condition 3 (psi)
Direction	P_x, P_y, P_z	P_x, P_y, P_z	P_x, P_y, P_z
1	-20.0,0.0,-5.0	-20.0,-5.0,0.0	-20.0,0.0,35.0
2	-20.0,0.0,-5.0	-20.0,-50.0,0.0	-20.0,0.0,0.0
3	-20.0,0.0,-30.0	-20.0,-5.0,0.0	-20.0,0.0,0.0
4	-20.0,0.0,-30.0	-20.0,-50.0,0.0	-20.0,0.0,-35.0

$A_{11}(5)A_{12} \sim A_{13}(6)A_{14} \sim A_{17}(7)A_{18} \sim A_{21}(8)A_{22} \sim A_{25}$ The truss members were subjected to the compression and tensile stress limitations shown in Table 9 In addition, maximum displacement limitations of ± 0.35 in were imposed on every node in every direction. The minimum cross-sectional area of all members was $0.01in^2$. In Fig.6 the convergence histories of a simple GA and H-SAGA are shown for the 25-bar truss. It could be seen that H-SAGA converges much faster and with fewer function evaluations and leads to better solution vectors compared to a simple GA. The neighbourhood search takes effect in as early as 20th generation, where it helps the algorithm detour from the course of the GA and find noticeably lower function values. Table 10 compares optimization results with those reported in literature.

3.6 The 72-bar space truss

The spatial 72-bar truss shown in Fig. 7 is a test case analyzed by many researchers (Schmit and Farshi [12], Schmit and Miura [13], Ven-kayya [14], Arora and Hauge [30], Chao et al. [31], Sedaghati [15], Farshi and Ziazi [21]). Material density is $0.1lb/in^3$ while the modulus of elasticity is $10000ksi$. The structure is subjected to two independent loading conditions.

1. Loading of $P_x = 5.0kips$, $P_y = 5.0kips$ and $P_z = -5.0kips$ imposed on node 17;
2. Loading of $P_z = -5.0kips$ is applied to nodes 17, 18, 19 and 20;

The loading condition divides the 72 member truss to these sub groupings: (1) $A_1 \sim A_4$ (2) $A_5 \sim A_{12}$ (3) $A_{13} \sim A_{16}$ (4) $A_{17} \sim A_{18}$ (5) $A_{19} \sim A_{22}$ (6) $A_{23} \sim A_{30}$ (7) $A_{31} \sim A_{34}$ (8) $A_{35} \sim A_{36}$ (9) $A_{37} \sim A_{40}$ (10) $A_{41} \sim A_{48}$ (11) $A_{49} \sim A_{52}$ (12) $A_{53} \sim A_{54}$ (13) $A_{55} \sim A_{58}$ (14) $A_{59} \sim A_{66}$ (15) $A_{67} \sim A_{70}$ (16) $A_{71} \sim A_{72}$.

The members were subjected to stress limitations of $\pm 25ksi$ and the maximum displacement of uppermost nodes was not allowed to exceed $\sim 0.25in$ in the x and y directions. In this case, the minimum cross-sectional area of all members was $0.1in^2$.

Optimization results are summarized in Table 11. It can be seen that the proposed algorithm outperforms other works presented in the literature.

3.6.1 The 200 bar truss structure with three independent loading conditions

The planar 200-bar truss, shown in Fig.8, sizing optimization problem was solved by Lamberti [29] and Farshi and Ziazi [21]. The steel members have a density of $0.283lb/in^3$ and modulus of elasticity $30000ksi$, respectively. There are only constraints on member stresses that must be lower than $10000psi$ (Same limit in tension and compression).

Table 7: Optimal design comparison for the 22-bar planar truss

Variables(in^2)	Sheu and Schmit [25]	Khan and Willmert [26]	Farshi and Ziazi [21]	This work
A_1	2.629	2.563	2.6250	2.6301
A_2	1.162	1.553	1.2164	1.2289
A_3	0.343	0.281	0.3466	0.3550
A_4	0.423	0.512	0.4161	0.4153
A_5	2.782	2.626	2.7732	2.7332
A_6	2.173	2.131	2.0870	2.0688
A_7	1.952	2.213	2.0314	2.0371
Weight(lb)	1024.8	1034.74	1023.9	1019.43

Note: $1 in^2 = 6.425cm^2$ $1lb = 4.448N$

Table 8: Loading conditions for the 25-bar space truss

Node	Loading Condition 1(kips)	Loading Condition 2(kips)
	P_x, P_y, P_z	P_x, P_y, P_z
1	0.0,20.0,-5.0	1.0,10.0,-5.0
2	0.0,-20.0,-5.0	0,10.0,-5.0
3	0.0,0.0,0.0	0.5,0.0,0.0
6	0.0,0.0,0.0	0.5,0.0,0.0

Table 9: Member stress limitations for the 25-bar space truss

Variables(in^2)	Compressive Stress Limitation (ksi)	Tensile stress limitation(ksi)
A_1	35.092	40.0
$A_2 \sim A_5$	11.590	40.0
$A_6 \sim A_9$	17.305	40.0
$A_{10} \sim A_{11}$	35.092	40.0
$A_{12} \sim A_{13}$	35.092	40.0
$A_{14} \sim A_{17}$	6.759	40.0
$A_{18} \sim A_{21}$	6.959	40.0
$A_{22} \sim A_{25}$	11.082	40.0

Table 10: Optimal design comparison for the 25-bar planar truss

Variables(in^2)	Schmit and Farshi [12]	Schmit and Miura [13]	Venkayya [14]	Adeli and Kamal [27]	Saka [28]	Lamberti [29]	Farshi and Ziazi [21]	This work
A_1	0.01	0.01	0.028	0.010	0.010	0.0100	0.0100	0.0100
A_2	1.964	1.985	1.964	1.986	2.085	1.9870	1.9981	1.9864
A_3	3.033	2.996	3.081	2.961	2.988	2.9935	2.9828	2.9975
A_4	0.01	0.01	0.01	0.010	0.010	0.0100	0.0100	0.0100
A_5	0.01	0.01	0.01	0.010	0.010	0.0100	0.0100	0.0100
A_6	0.67	0.684	0.693	0.806	0.696	0.6840	0.6837	0.6806
A_7	1.68	1.667	1.678	1.680	1.670	1.6769	1.6750	1.6733
A_8	2.67	2.662	2.627	2.530	2.592	2.6621	2.6668	2.6638
Weight(lb)	545.22	545.17	545.49	545.66	545.23	545.16	545.37	544.88

Note: $1 in^2 = 6.425cm^2$ $1lb = 4.448N$

Table 11: Optimal design comparison for the 72-bar space truss

Variables(in^2)	Schmit and Farshi [12]	Schmit and Miura [13]	Venkayya [14]	Arora and Haug [30]	Chao et al. [31]	Sedaghati [15]	Farshi and Ziazi [21]	This work
A_1	0.158	0.157	0.161	0.1564	0.157	0.1565	0.1565	0.1563
A_2	0.594	0.546	0.557	0.5464	0.549	0.5456	0.5457	0.5462
A_3	0.341	0.411	0.377	0.4110	0.406	0.4104	0.4106	0.4096
A_4	0.608	0.570	0.506	0.5712	0.555	0.5697	0.5697	0.5696
A_5	0.264	0.523	0.611	0.5263	0.513	0.5237	0.5237	0.5239
A_6	0.548	0.517	0.532	0.5178	0.529	0.5171	0.5171	0.5159
A_7	0.100	0.100	0.100	0.1000	0.100	0.1000	0.1000	0.1002
A_8	0.151	0.100	0.100	0.1000	0.100	0.1000	0.1000	0.1006
A_9	1.107	1.267	1.246	1.2702	1.252	1.2684	1.2685	1.2691
A_{10}	0.579	0.512	0.524	0.5124	0.524	0.5117	0.5118	0.5101
A_{11}	0.100	0.100	0.100	0.1000	0.100	0.1000	0.1000	0.1000
A_{12}	0.100	0.100	0.100	0.1000	0.100	0.1000	0.1000	0.1012
A_{13}	2.078	1.885	1.818	1.8656	1.832	1.8862	1.8864	1.8861
A_{14}	0.503	0.513	0.524	0.5131	0.512	0.5123	0.5122	0.5129
A_{15}	0.100	0.100	0.100	0.1000	0.100	0.1000	0.1000	0.1000
A_{16}	0.100	0.100	0.100	0.1000	0.100	0.1000	0.1000	0.1009
Weight(lb)	388.63	379.64	381.2	379.62	379.62	379.62	379.65	379.56

Note: $1 in^2 = 6.425cm^2$ $1lb = 4.448N$

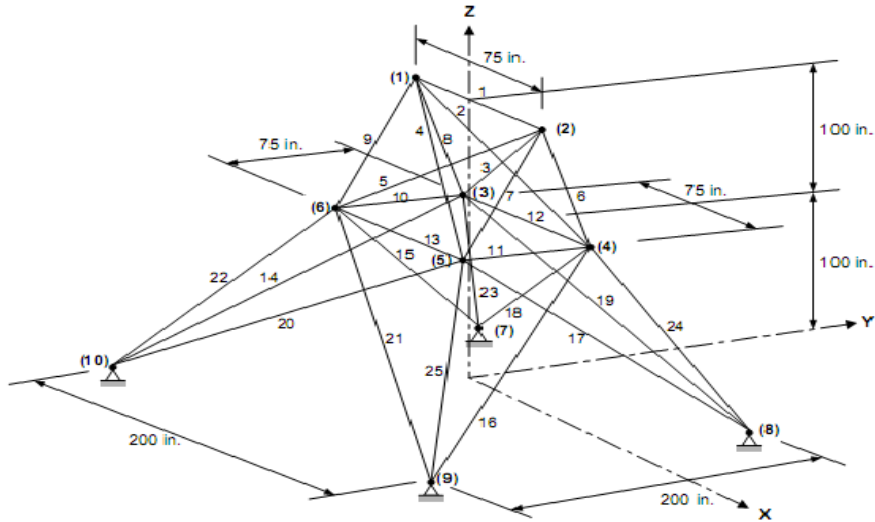


Figure 5: 25-bar space truss

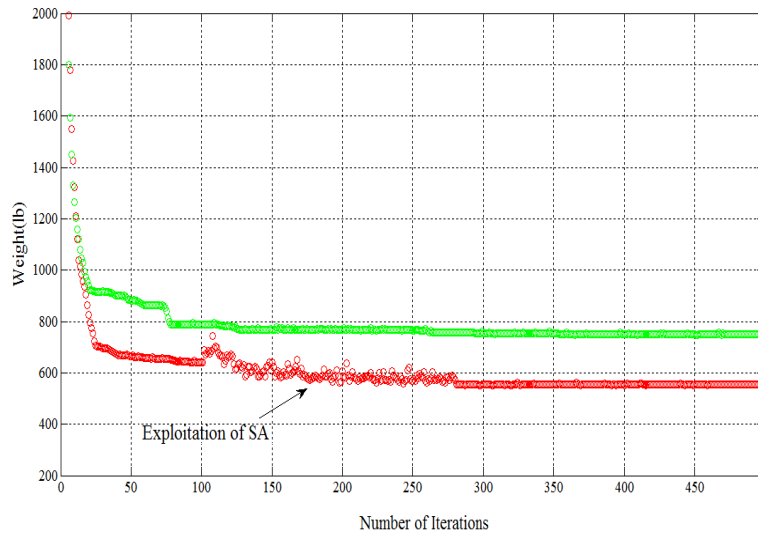


Figure 6: The 25-bar convergence history

The structure is subjected to three independent loading condition:

(a) 1000lb in positive x - direction at nodes 1, 6, 15, 20, 29, 43, 48, 57, 62 and 71;

(b) 10000lb in negative y - direction at nodes 1, 2, 3, 4, 5, 6, 8, 10, 12, 14, 15, 16, 17, 18, 19, 20, 22, 24, 26, 28, 29, 30, 31, 32, 33, 34, 36, 38, 40, 42, 43, 44, 45, 46, 47, 48, 50, 52, 54, 56, 58, 59, 60, 61, 62, 64, 66, 68, 70, 71, 72, 73, 74 and 75;

(c) The loading conditions (a) and (b) acting together.

Groupings were done in order to have 200 independent variables. Table 12 compares optimization results with literature. In Fig.9 the convergence histories of a simple GA and H-SAGA are shown for the 200-bar truss. Again, it could be seen that H-SAGA converges much faster and with fewer function evaluations and leads to better solution vectors. This time the detour begins in about 120th generation.

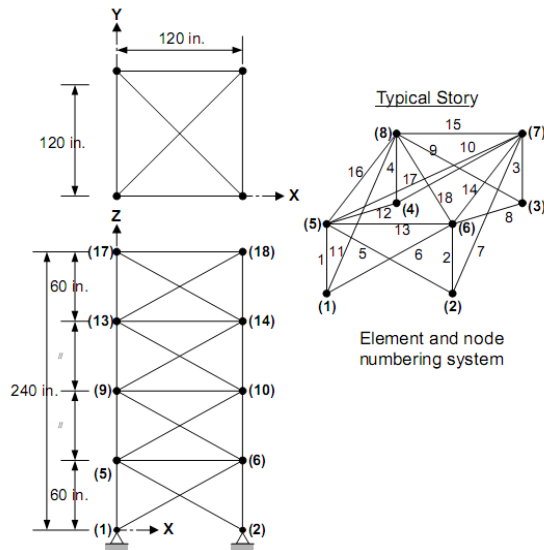
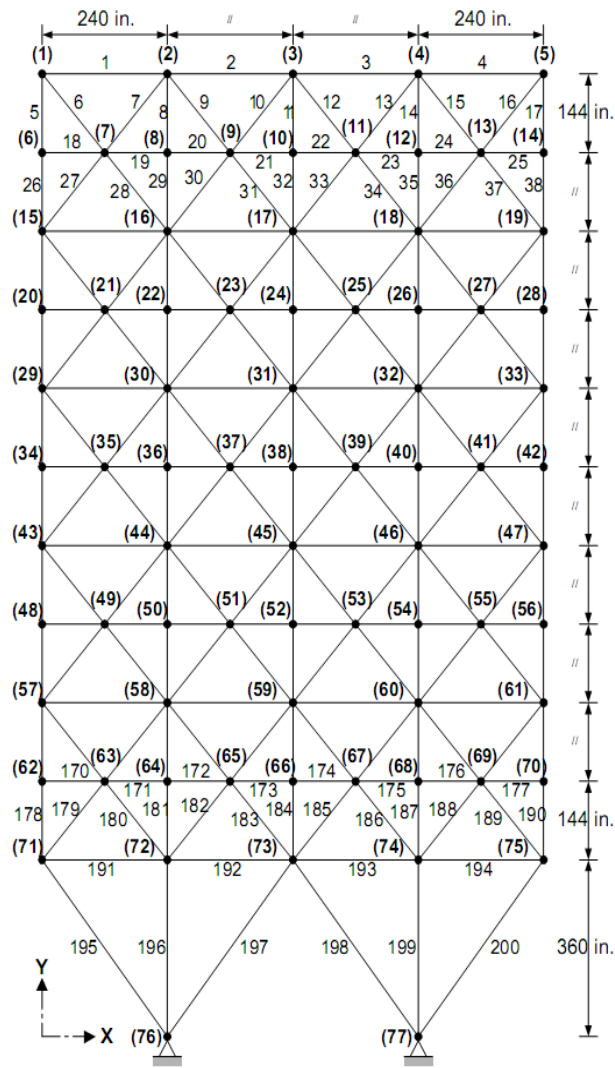


Figure 7: 72-bar space truss



Note: For the sake of clarity, not all members are numbered in this figure.

Figure 8: 200-bar space truss

Table 12: Optimal design comparison for the 200-bar planar truss

Variables(in^2)	Members	Lamberti [29]	Farshi and Ziazi [21]	This work
A_1	1,2,3,4	0.1467	0.147	0.1457
A_2	5,8,11,14,17	0.94	0.945	0.9405
A_3	19,20,21,22,23,24	0.1	0.1	0.1004
A_4	18,25,56,63,94,101,132,139,170,177	0.1	0.1	0.1
A_5	26,29,32,35,38	1.94	1.9451	1.9397
A_6	6,7,9,10,12,13,15,16,27,28,30,31,33,34,36,37	0.2962	0.2969	0.2958
A_7	39,40,41,42	0.1	0.1	0.101
A_8	43,46,49,52,55	3.104	3.1062	3.1032
A_9	57,58,59,60,61,62	0.1	0.1	0.1012
A_{10}	64,67,70,73,76	4.104	4.1052	4.1084
A_{11}	44,45,47,48,50,51,53,54,65,66,68,69,71,72,74,75	0.4034	0.4039	0.4042
A_{12}	77,78,79,80	0.1922	0.1934	0.1872
A_{13}	81,84,87,90,93	5.4282	5.4289	5.4329
A_{14}	95,96,97,98,99,100	0.1	0.1	0.1018
A_{15}	102,105,108,111,114	6.4282	6.4289	6.4244
A_{16}	82,83,85,86,88,89,91,92,103,104,106,107,109,110,112,113	0.5738	0.5745	0.5723
A_{17}	115,116,117,118	0.1325	0.1339	0.1327
A_{18}	119,122,125,128,131	7.9726	7.9737	7.9708
A_{19}	133,134,135,136,137,138	0.1	0.1	0.1007
A_{20}	140,143,146,149,152	8.9726	8.9737	8.9735
A_{21}	120,121,123,124,126,127,129,130,141,142,144,145,147,148,150,151	0.7048	0.7053	0.7048
A_{22}	153,154,155,156	0.4202	0.4215	0.4192
A_{23}	157,160,163,166,169	10.8666	10.8675	10.8671
A_{24}	171,172,173,174,175,176	0.1	0.1	0.1002
A_{25}	178,181,184,187,190	11.8666	11.8674	11.8649
A_{26}	158,159,161,162,164,165,167,168,179,180,182,183,185,186,188,189	1.0344	1.0349	1.0333
A_{27}	191,192,193,194	6.6838	6.6849	6.6852
A_{28}	195,197,198,200	10.8083	10.8101	10.8036
A_{29}	196,199	13.8339	13.8379	13.8328
Weight(lb)	25446.76	25456.57	25443.11	

Note: $1 in^2 = 6.425cm^2$, $1lb = 4.448N$

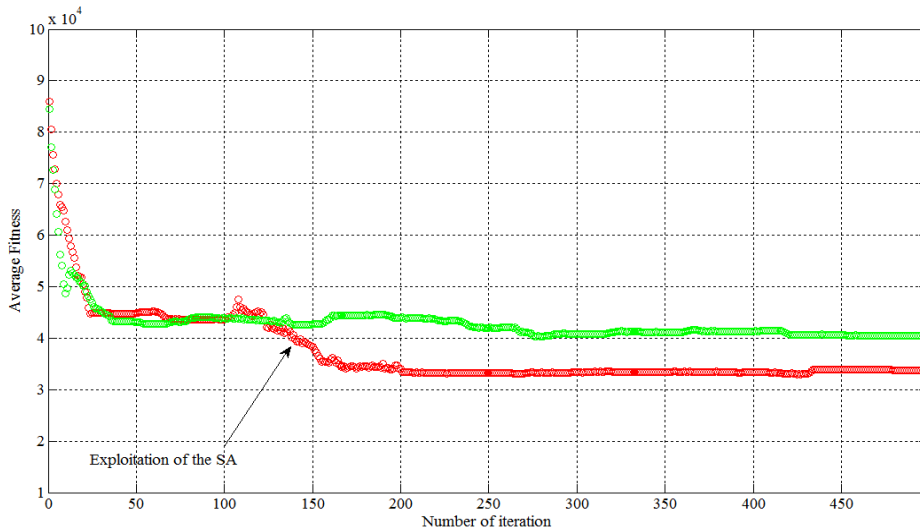


Figure 9: The 200-bar convergence history

3.6.2 The 200 bar truss structure with five independent loading conditions

The planar 200-bar truss structure shown in Fig.8 can be optimized also with 200 design variables by assigning a sizing variable to the cross-sectional of each element. The structure is designed to carry five independent loading conditions. Besides the three load cases listed in Section 3.6.1, the structure is also loaded by (d)1000 lb f acting in the negative x – direction at node points 5, 14, 19, 28, 33, 42, 47, 56, 61, 70 and 75;

(e) Loading conditions (b) and (d) described in section 3.6.1 acting together.

The optimization problem includes 3500 non-linear constraints on nodal displacements and member stresses. The displacements of all free nodes in both directions x and y must be less than $\pm 0.5in$. The allowable stress (the same in tension and compression) is 30000 psi . The lower bound of cross-sectional areas is $0.1in^2$. The latest and the best optimal result reported by Lamberti and Pappalettere[32] is 28781 lb but H-SAGA outperforms it by obtaining 28661 lb for the weight of this structure.

3.7 The 112-bar dome truss

Fig.10 shows the 112-bar steel dome that has been previously discussed in Saka [28] and Erbatur and Hasancebi [33]. The optimization problem is modified as follows. First, 112 members of the dome are collected in seven distinct groups,

Table 13: Loading condition for the 112-bar dome

Joint's number	$x(kips)$	$y(kips)$	$z(kips)$
1	0	5	12
17,23,29,35	0	9	9
16,18,22,24, 28,30,31,32	8	7	7
others	8	7	9

Table 14: Optimal design comparison for the 112- bar dome truss

Variables(in^2)	Erbatur [33]	This work
A_1	1.095	1.059
A_2	0.863	0.888
A_3	1.033	0.929
A_4	1.095	0.948
A_5	1.095	1.024
A_6	0.81	0.9
A_7	1.735	1.612
Weight(lb)	7657.778	7015.053

Note: $1 in^2 = 6.425cm^2$ $1lb = 4.448N$

while two groups were used in Saka[28]. Next, in place of *AISC* specification, the allowable compressive stress for each member is computed according to the Turkish specification. Despite the fact that the Turkish specification leads to safer values in computing the allowable compressive stresses, the distinction is not of much consequence. Loading conditions and optimization results are respectively presented in Table 13 and 14. Complete detailed list of design data is presented as follow:

Displacement constraints: $\delta_j \leq 20mm$ in z direction, $j = 1, 17, 23$;

Stress constraints: $\sigma_{tension_i} \leq 34.8ksi$, $\sigma_{compression_i} \leq TURKISH spec, i = 1, \dots, 112$;

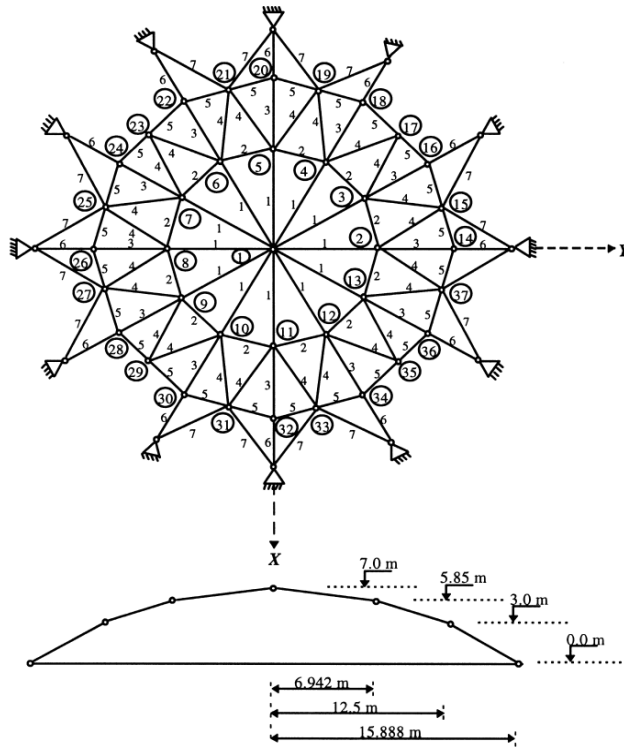


Figure 10: The 112-bar dome truss

3.8 The 132-bar geodesic dome

Fig. 11 shows a geodesic truss dome consisting of 132 bar elements that has been analyzed by Farshi and Ziazi [21]. Stress limitations for all members is $25ksi$. Cross sectional areas must be greater than $0.1in^2$. The areas are linked together to form 36 independent design variables (Table 16). Bottom nodes are fixed to ground in all coordinate directions while free nodes cannot displace by more than $0.1in$. The structure is subject to four independent loading

Table 15: Loading conditions for the 132-bar geodesic dome
 Loaded joints 1000 lb downward acts on each node

1	$A_1 \sim A_4$
2	$A_5 \sim A_6$
3	$A_7 \sim A_8$
4	$A_9 \sim A_{10}$

Table 16: Optimal design comparison for the 132-bar geodesic dome

Variables(in^2)	Members	Farshi and Ziazi [21]	This work	Variables	Members	Farshi and Ziazi [21]	This work
A_1	3,6	0.9876	0.9915	A_{19}	44,47,59,62	0.3910	0.3834
A_2	1,2,4,5	0.9902	0.9834	A_{20}	45,46,60,61	0.4597	0.455
A_3	8,9,11,12	0.9041	0.899	A_{21}	78,79,87,88	0.2128	0.212
A_4	7,10	0.8509	0.8495	A_{22}	77,80,86,89	0.1721	0.1713
A_5	19,28	0.3703	0.3692	A_{23}	76,81,85,90	0.2264	0.2275
A_6	18,20,27,29	0.4920	0.4852	A_{24}	73,75,82,84	0.1657	0.1624
A_7	17,21,26,30	0.4145	0.4101	A_{25}	74,83	0.1000	0.101
A_8	13,16,22,25	0.5519	0.5452	A_{26}	105,126	0.1000	0.1041
A_9	14,15,23,24	0.5110	0.5052	A_{27}	104,106,125,127	0.3229	0.3223
A_{10}	34,35,40,41	0.4278	0.4225	A_{28}	103,107,124,128	0.3228	0.3167
A_{11}	33,36,39,42	0.4565	0.459	A_{29}	102,108,123,129	0.4175	0.4144
A_{12}	31,32,37,38	0.3808	0.3722	A_{30}	101,109,122,130	0.2587	0.256
A_{13}	53,68	0.3115	0.3087	A_{31}	100,110,121,131	0.4973	0.4911
A_{14}	52,54,67,69	0.3826	0.3772	A_{32}	99,111,120,132	0.2660	0.267
A_{15}	51,55,66,70	0.3804	0.375	A_{33}	91,98,112,119	0.1000	0.1001
A_{16}	50,56,65,71	0.4412	0.4385	A_{34}	92,97,113,118	0.3394	0.338
A_{17}	49,57,64,72	0.3359	0.3337	A_{35}	93,96,114,117	0.3425	0.3434
A_{18}	43,48,58,63	0.5058	0.5083	A_{36}	94,95,115,116	0.2986	0.2967
					Weight (lb)	172.74	171.52

Note: $1 in^2 = 6.425cm^2$ $1lb = 4.448N$

conditions (Table 15). Optimization results are summarized in Table 16.

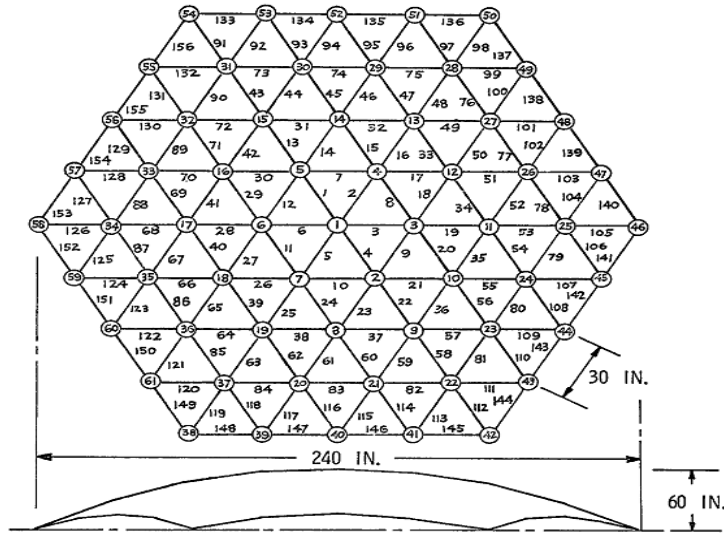


Figure 11: The 132-bar dome truss

3.9 The 26-story tower truss

The 26-story-tower space truss containing 942 elements and 244 nodes is considered in this section. 59 design variables are used to represent the cross-sectional areas of 59 element groups in this structure because of structural symmetry. Figures 12 and 13 show the geometry and the 59 element groups. The material density is $0.1lb/in^3$ and the modulus of elasticity is $10000ksi$. The members are subject to the stress limit of $\pm 25ksi$ ($\pm 172.375MPa$) and the four nodes of the top level in the x , y and z directions are subject to the displacement limits of $\pm 15.0in$ ($\pm 38.10cm$) (about $1/250$ of the total height of the tower). The allowable cross-sectional areas in this example are selected from 0.1 to $20.0in^2$ (0.6452 to $129.03cm^2$). The loading on the structure consists of:

- (1) The vertical load at each node in the first section is equal to $3kips$;
- (2) The vertical load at each node in the second section is equal to $6kips$;
- (3) The vertical load at each node in the third section is equal to $9kips$;
- (4) The horizontal load at each node on the right side in the x direction is equal to $1kips$;
- (5) The horizontal load at each node on the left side in the x direction is equal to $1.5kips$;
- (6) The horizontal load at each node on the front side in the y direction is equal to $1kips$;
- (7) The horizontal load at each node on the back side in the y direction is equal to $1kips$;

Table 17 compares optimization results with literature.

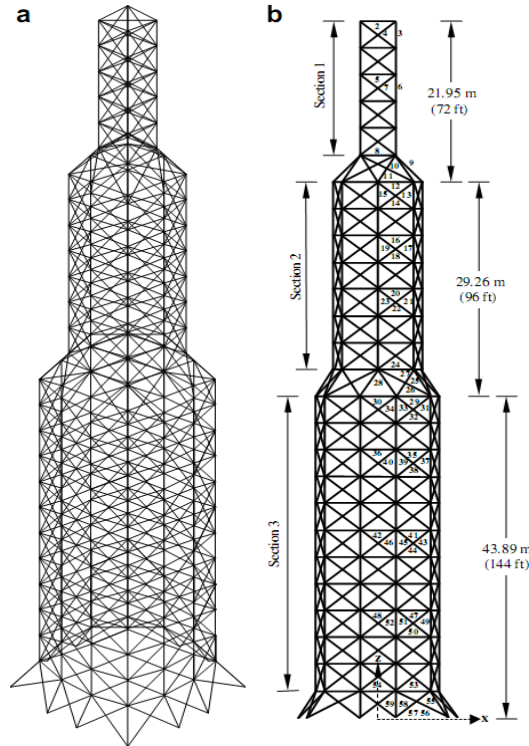


Figure 12: The 26-Story, 942-bar space truss tower: (a) 3D view, and (b) Side view

4 Conclusion

A new hybrid algorithm, H-SAGA, was presented for the optimal design of planar- and space truss structures. The Genetic-based algorithm features a local-search engine that benefits from a Simulated Annealing-like stochastic search scheme. The algorithm was further “tuned”, e.g. by adopting a dynamic local search strategy, to better suit the complex nature of the problem at hand. Ten different structures, including a 112 member dome truss and a 26-story tower truss were optimally designed using the proposed algorithm and the results were compared with those reported in the literature (wherever available). The comparison showed that H-SAGA outperformed other algorithms, in some cases noticeably, both in terms of solution optimality and computational cost. In addition to its fairly high convergence rate which causes computational efficiency, the proposed algorithm is distinguished by its ability to fluently escape the traps of the local minima and to carefully avoid constraint violations when different random initial points are used.

Table 17: Optimal design comparison for the 26-story tower truss

Cross Section(in^2)	Erbatur and Hasancebi [33]	Hasancebi [34]	This work
A_1	1	1.02	3.3409
A_2	1	1.037	1.0226
A_3	3	2.943	5.7605
A_4	1	1.92	2.4798
A_5	1	1.025	1.0000
A_6	17	14.961	14.3539
A_7	3	3.074	2.8752
A_8	7	6.78	11.7044
A_9	20	18.58	14.8708
A_{10}	1	2.415	3.6599
A_{11}	8	6.584	5.1913
A_{12}	7	6.291	5.5767
A_{13}	19	15.383	14.1554
A_{14}	2	2.1	2.1912
A_{15}	5	6.021	2.9070
A_{16}	1	1.022	1.0000
A_{17}	22	23.099	18.1769
A_{18}	3	2.889	2.5274
A_{19}	9	7.96	12.6091
A_{20}	1	1.008	1.0361
A_{21}	34	28.548	31.1194
A_{22}	3	3.349	2.8803
A_{23}	19	16.144	17.0459
A_{24}	27	24.822	18.3234
A_{25}	42	38.401	38.7810
A_{26}	1	3.787	2.6226
A_{27}	12	2.32	9.2714
A_{28}	16	17.036	13.0850
A_{29}	19	14.733	13.5173
A_{30}	14	15.031	16.3403
A_{31}	42	38.597	37.3477
A_{32}	4	3.511	3.1946
A_{33}	4	2.997	6.3378
A_{34}	4	3.06	1.8829
A_{35}	1	1.086	1.0000
A_{36}	1	1.462	1.1151
Weight(lb)	143436	141241	140674

Note: $1 in^2 = 6.425cm^2$ $1lb = 4.448N$

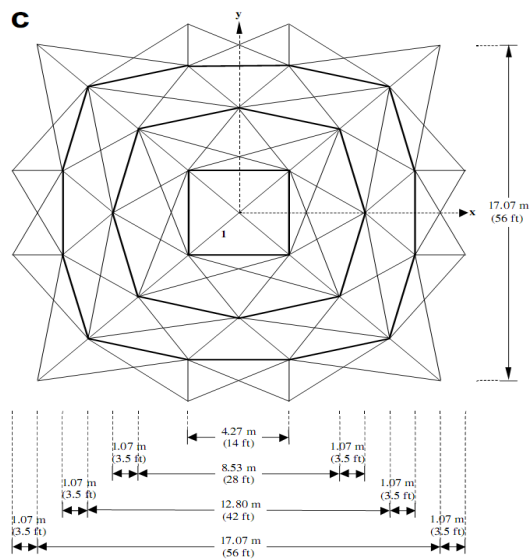


Figure 13: The 26-Story, 942-bar space truss tower: (c) Top view

References

- [1] S. N. Sivanandam and S. N. Deepa. *Introduction to Genetic Algorithms*. Springer Berlin Heidelberg, New York, 2008.
- [2] John H. Holland. *Adaptation in Natural and Artificial Systems*. MIT press, Cambridge, 1992.
- [3] A. Bolte and U.W. Thonemann. Theory and methodology of optimizing simulated annealing schedules with genetic programming. *European Journal of Operational Research*, 92:402–416, 1996.
- [4] Z.G Wang, Y.S Wong, and M. Rahman. Optimization of multi-pass milling using genetic algorithm and genetic simulated annealing. *The International Journal of Advanced Manufacturing Technology*, 24:727–732, 2004.
- [5] Z. Wren, Y. San, and J. F. Chen. Hybrid simplex-improved genetic algorithm for global numerical optimization. *Acta Automotica Sinica*, 33:91–95, 2007.
- [6] H. Rahami, A. Kaveh, M. Aslani, and R. Najian Asl. A hybrid modified genetic-nelder mead simplex algorithm for large-scale truss optimization. *Int. J. Optim. Civil Eng.*, 1:29–46, 2011.
- [7] M. Aslani, R. Najian Asl, R. Oftadeh, and M. Shariat Panahi. A novel hybrid simplex-genetic algorithm for the optimum design of truss structures. In *Proceedings of the World Congress on Engineering 2010 Vol II*, 2010.
- [8] S. Erkoc N. Dugan. Genetic algorithm-monte carlo hybrid geometry optimization method for atomic clusters. *Computational Materials Science*, 45:127–132, 2009.
- [9] S. K. S. Fan, Y. C. Liang, and E. Zahara. A genetic algorithm and a particle swarm optimizer hybridized with neldermead simplex search. *Computers & Industrial Engineering*, 50:401–425, 2006.
- [10] O. Hasancebi, S. Carbas, and M.P Saka. Improving the performance of simulated annealing in structural optimization. *Structural and Multidisciplinary Optimization*, 41:189–203, 2010.
- [11] S. Kirkpatrick and M. P. Vecchi Jr C. D. Gelatt. Optimization by simulated annealing. *Science Journal*, 220:671–699, 1983.
- [12] L.A. Schmit and B. Farshi. Some approximation concepts for structural synthesis. *AIAA Journal*, 12:692–699, 1974.
- [13] L.A. Schmit and H. Miura. Approximation concepts for efficient structural synthesis. *NASA-CR-2552*, 1:163–168, 1976.
- [14] V.B Venkayya. Design of optimum structures. *Computers and Structures*, 1:265–309, 1971.
- [15] R. Sedaghati. Benchmark case studies in structural design optimization using the force method. *International Journal of Solids and Structures*, 42:5848–5871, 2005.
- [16] A. Kaveh and H. Rahami. Analysis, design and optimization of structures using force method and genetic algorithm. *International Journal for Numerical Methods in Engineering*, 65:1570–1584, 2006.
- [17] L. J. Li, Z. B. Huang, F. Liu, and Q. H. Wu. A heuristic particle swarm optimizer for optimization. *Computers and Structures*, 85:340–349, 2007.
- [18] P. Rizzi. Optimization of multi-constrained structures based on optimality criteria. In *Proceedings of the AIAA/ASME/SAE 17th Structures Structural Dynamics and Materials Conference*, pages 448–462, May 1976.
- [19] K. V. John, C. V Ramakrishnan, and KG. Sharma. Minimum weight design of trusses using improved move limit method of sequential linear programming. *Computers and Structures*, 27:583–591, 1987.
- [20] K. S. Lee and Z. W. Geem. A new structural optimization method based on the harmony search algorithm. *Computers and Structures*, 82:781–798, 2004.
- [21] B. Farshi and A. Ziazi. Sizing optimization of truss structures by method of centers and force formulation. *International Journal of Solids and Structures*, 47:2508–2524, 2010.
- [22] V. B. Venkayya, N. S. Khot, and L. Berke. *Application of Optimality Criteria Approaches to Automated Design of Large Practical Structures*. AGARD-CP-123, 1973.
- [23] H. Adeli and S. Kumar. Distributed genetic algorithm for structural optimization. *J Aerospace Eng, ASCE*, 8,3:156–163, 1995.
- [24] K. Imai and L. A. Schmit. Configuration optimization of trusses. *J Structural Division, ASCE*, 107:745–756, 1981.
- [25] C. Y. Sheu and L. A. Schmit. Minimum weight design of elastic redundant trusses under multiple static load conditions. *AIAA Journal*, 10:155–162, 1972.
- [26] M. R. Khan, K. D. Willmert, and W. A. Thornton. An optimality criterion method for large-scale structures. *AIAA Journal*, 17:753–761, 1979.
- [27] H. Adeli and O. Kamal. Efficient optimization of space trusses. *Computers and Structures*, 24:501–511, 1986.
- [28] MP. Saka. Optimum design of pin-jointed steel structures with practical applications. *J Struct Eng. ASCE*, 116, 10:2599–2620, 1990.
- [29] L. Lamberti. An efficient simulated annealing algorithm for design optimization of truss structures. *Computers and Structures*, 86:1936–1953, 2008.
- [30] JR. Haug J. S Arora. Efficient optimal design of structures by generalized steepest descent programming. *International Journal for Numerical Methods in Engineering*, 10:747766, 1976.
- [31] N. H. Chao, S. J. Fenves, and A. W. Westerberg. *Application of reduced quadratic programming technique to optimal structural design*. John Wiley, New York, 1984.

- [32] Lamberti and Pappalettere. Move limits definition in structural optimization with sequential linear programming, part ii: Numerical examples. *Computer and Structures*, 81:215–238, 2003.
- [33] F. Erbaturo and O. Hasancebi. Optimal design of planar and space structures with genetic algorithms. *Computer and Structures*, 75:209–224, 2000.
- [34] O. Hasancebi. Adaptive evolution strategies in structural optimization: Enhancing their computational performance with applications to large-scale structures. *Computers and Structures*, 86:119–132, 2008.